Mechanistic Imperatives for Catalysis of Aldol Addition Reactions: Partitioning of the Enolate Intermediate between Reaction with Brønsted Acids and the Carbonyl Group

John P. Richard*,[1] and R. W. Nagorski[†]

Contribution from the Department of Chemistry, University at Buffalo, SUNY, Buffalo, New York 14260-3000

Received January 4, 1999

Abstract: The lyoxide ion catalyzed intramolecular aldol addition reaction of 2-(2-oxopropyl)benzaldehyde (**1**) to give the aldol adduct **3** proceeds via essentially irreversible formation of the acetone-like enolate intermediate **2**, because reprotonation of **2** by a solvent of H_2O or D_2O (k_{HOH} or k_{DOD}) is much slower than intramolecular addition of the enolate to the carbonyl group (k_c). The aldol addition reaction of **1** catalyzed by high concentrations of 3-substituted quinuclidine buffers proceeds via reversible deprotonation of **1** to give the enolate **2**, and rate-determining addition of the enolate to the carbonyl group. A rate constant ratio of $k_c/k_{HOH} = 35$ was determined for partitioning of the enolate **2** between intramolecular addition to the carbonyl group and protonation by solvent water. The corresponding ratios k_{BH}/k_c (M^{-1}) for the protonation of **2** by Brønsted buffer acids and intramolecular aldol addition increase from 7 to 450 as the acidity of the buffer acid is increased from $pK_{BH} = 11.5$ to 7.5. The data show that the electrophilic reactivity of the benzaldehyde carbonyl group toward intramolecular addition of the enolate **2** is the same as that of a hypothetical tertiary ammonium cation of $pK_{BH} = 13.3$. The Marcus intrinsic barrier for addition of the enolate **2** to the carbonyl group is unexpectedly small, which suggests that the transition state for this reaction is stabilized by interactions between the soft−soft acid−base pair. The relevance of this work to chemical and enzymatic catalysis of aldol condensation reactions is discussed.

The direct determination of rate constants for the protonation of simple enolates by solvent water (k_{HOH}) and buffer catalysts (k_{BH}) have provided a detailed description of substituent effects on the reactivity of these carbanions.[2] Similarly, the addition of enolates to carbonyl electrophiles in water, a reaction that occurs broadly in chemical[3a] and biochemical[3b] syntheses of carbon−carbon bonds, has been examined in Guthrie's laboratory and estimates of rate constants, k_c, for these reactions reported.[4−6]

While rate constants k_{BH} and k_c (Scheme 1) have been determined or estimated in separate experimental studies of the reactions of a variety of enolates with a variety of Brønsted acids and carbonyl groups (Scheme 1), we are not aware of any attempts to quantify these rate constants by directly monitoring the partitioning of a simple enolate between protonation and addition to the carbonyl group. The present experiments were initiated to obtain a precise determination of the relative electrophilicity of Brønsted acids and the carbonyl group

Scheme 1

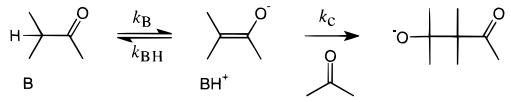

(k_{BH}/k_c) toward a simple enolate, by determining directly the relative rates for partitioning of an enolate between reaction with these electrophiles. Such kinetic studies have a broad significance in chemistry and biology.

1. The magnitude of k_{BH}/k_c determines the yield of the aldol adduct from partitioning of an enolate between protonation and addition to the carbonyl group in water, so that good yields of the aldol adduct will be obtained from the reaction of an enolate in water when this rate constant ratio is small.[7,8]

2. The rate-limiting step for aldol addition depends on the relative barriers to partitioning of the enolate intermediate between protonation (k_{BH}) and addition to the carbonyl group (k_c). When $k_c \gg k_{BH}$, deprotonation of the substrate to give the enolate, k_B, is effectively irreversible and therefore rate-determining for the overall aldol addition reaction. However, when $k_{BH} \gg k_c$, the observed rate constant for aldol addition will depend on k_c, and the reaction will be accelerated by reagents that lower the barrier to this rate-limiting step. Therefore, a knowledge of the rate-determining step for aldol addition is important for the design of simple chemical catalysts

[†] Current address: Department of Chemistry, Illinois State University, Normal, IL 61790-4160.

(1) Tel: (716) 645 6800 ext. 2194. Fax: (716) 645 6963. E-mail: jrichard@chem.buffalo.edu.

(2) Keeffe, J. R.; Kresge, A. J. In *The Chemistry of Enols*; Rappoport, Z., Ed.; Wiley: Chichester, UK, 1990; pp 399−480.

(3) (a) Heathcock, C. H. In *Asymmetric Synthesis*; Morrison, J. D., Ed.; Academic Press: New York, 1984; Vol. 3; pp 111−212. (b) Takayama, S.; McGarvey, G. J.; Wong, C.-H. *Annu. Rev. Microbiol.* **1997**, *51*, 285−310.

(4) Guthrie, J. P. *J. Am. Chem. Soc.* **1991**, *113*, 7249−7255.

(5) Guthrie, J. P.; Guo, J. *J. Am. Chem. Soc.* **1996**, *118*, 11472−11487.

(6) Guthrie, J. P.; Barker, J. A. *J. Am. Chem. Soc.* **1998**, *120*, 6698−6703.

(7) Bartlett, P. A.; Satake, K. *J. Am. Chem. Soc.* **1988**, *110*, 1628−1630.

(8) Bartlett, P. A.; McLaren, K. L.; Marx, M. A. *J. Org. Chem.* **1994**, *59*, 2082−2085.

10.1021/ja9900297 CCC: $18.00
Published on Web 05/07/1999

of this reaction,[9] and to an understanding of the imperatives for the catalysis of aldol addition by enzymes[10] and enzyme mimics.[11]

3. The determination of k_{BH}/k_c will provide an accurate value for the *relative* Marcus intrinsic barriers for partitioning of an enolate between reaction with Brønsted acids and the carbonyl group,[4,5] provided the relative thermodynamic driving force for reaction with the two electrophiles is also known.

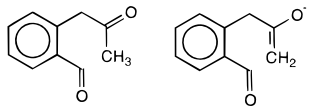

It is difficult to obtain and interpret rate data for bimolecular aldol addition because these reactions do not proceed cleanly toward formation of a single stable product, but rather give a complex mixture of unstable products.[12] By contrast, intramolecular aldol addition reactions can be designed to proceed cleanly toward formation of a single stable product.[5,13] We have shown that the intramolecular aldol condensation reaction of **1** at low concentrations (0.10−1.0 mM) proceeds through the enolate intermediate **2** to give a good yield of 2-naphthol (**4**).[13] Analysis of the kinetic data for aldol addition and for the initial deprotonation of **1** allows for the determination of rate constant ratios k_{BH}/k_c for partitioning of the enolate **2** between protonation by Brønsted acids and intramolecular addition to the carbonyl group. These results provide a quantitative description of the relative electrophilicities of Brønsted acids and the carbonyl group toward a simple enolate, and insight into the imperatives for catalysis of aldol addition by enzymes and enzyme mimics.

Experimental Section

Materials. 2-Indanone, methylmagnesium iodide, 3-quinuclidinone hydrochloride, 3-quinuclidinol, 3-chloroquinuclidine hydrochloride, quinuclidine hydrochloride, and potassium deuterioxide (40 wt %, 98+% D) were from Aldrich. Deuterium oxide (99.9% D), deuterium chloride (35% w/w, 99.5% D), and $CDCl_3$ (99.8% D) were from Cambridge Isotope Laboratories. The 3-substituted quinuclidines were purified by recrystallization from the following solvents: 3-quinuclidinone hydrochloride, ethanol/water; 3-quinuclidinol, acetone; 3-chloroquinuclidine hydrochloride, methanol/water; quinuclidine hydrochloride, ethanol. All other chemicals were reagent grade and were used without further purification. The water used for kinetic and HPLC studies was distilled and then passed through a Milli-Q water purification system. The procedures for the preparation of 2-(2-oxopropyl)-benzaldehyde (**1**) from 2-indanone and for the preparation of solutions for kinetic studies are described in the Supporting Information.

Deuterium Exchange Reactions of 1. The deuterium exchange reactions of **1** ([S] = 3.5−5 mM) in D_2O at 25 °C and I = 1.0 (KCl) were monitored by ^{1}H NMR spectroscopy,[14,15] using the procedures described in the Supporting Information.

^{1}H NMR spectra were recorded in $CDCl_3$ at 25 °C on a Varian VXR-400S spectrometer. Chemical shifts were referenced to $CHCl_3$ at 7.27 ppm. Relaxation times of the α-CH_2 and α-CH_3 protons of **1** were determined to be in the range T_1 = 4−6 s. Spectra (32−64 transients, 60 s relaxation delay) were obtained using a sweep width of 5300 Hz, a 90° pulse angle, and an acquisition time of 6 s.

The exchange for deuterium of the first benzylic proton of **1** in D_2O was followed by monitoring the disappearance of the singlet at 4.146 ppm due to the α-CH_2 group and the appearance of the triplet due to the α-CHD group which is shifted 0.028 ppm upfield from the singlet. Reaction progress, R_{CH_2}, was calculated using eq 1,[16] where A_{CH_2} and A_{CHD} are the integrated areas of the singlet and triplet for the α-CH_2 and α-CHD groups, respectively. The exchange for deuterium of the first proton of the α-CH_3 group of **1** in D_2O was followed by monitoring the disappearance of the singlet at 2.327 ppm due to the α-CH_3 group and the appearance of the triplet due to the α-CH_2D group which is shifted 0.016 ppm upfield from the singlet. Reaction progress, R_{CH_3}, was calculated using eq 2,[16] where A_{CH_3} and A_{CH_2D} are the integrated areas of the singlet and triplet for the α-CH_3 and α-CH_2D groups, respectively.

Semilogarithmic plots (not shown) of R_{CH_2} or R_{CH_3} against time according to eqs 3 and 4 were linear during exchange for deuterium of up to 35% of the first proton of the α-CH_2 or the α-CH_3 group of **1**. The negative slopes of the former plots are equal to the statistically corrected rate constant $k_{obsd}/2$ for reaction of a single proton of the α-CH_2 group of **1**, where k_{obsd} is the rate constant for exchange of the *first* proton of the α-CH_2 group (eq 3).[16] The negative slopes of the latter plots are equal to the statistically corrected rate constant $k_{obsd}/3$ for reaction of a single proton of the α-CH_3 group of **1**, where k_{obsd} is the rate constant for exchange of the *first* proton of the α-CH_3 group (eq 4).[16] The values of k_{obsd} were reproducible to ±10%.

$$R_{CH_2} = \frac{A_{CH_2}}{A_{CH_2} + A_{CHD}} \quad (1)$$

$$R_{CH_3} = \frac{A_{CH_3}}{A_{CH_3} + \frac{A_{CH_2D}}{2}} \quad (2)$$

$$\ln R_{CH_2} = -k_{obsd}t/2 \quad (3)$$

$$\ln R_{CH_3} = -k_{obsd}t/3 \quad (4)$$

Aldol Condensation Reactions of 1. All reactions were carried out at 25 °C and ionic strength 1.0 (KCl). Reactions were initiated by making a 2500-fold dilution of a solution of **1** in acetonitrile into 3 mL of the appropriate reaction mixture to give a final substrate concentration of 0.1−0.3 mM. Rate constants for the conversion of **1** to 2-naphthol (**4**) were determined spectrophotometrically by following

(9) Chaperon, A. R.; Engeloch, T. M.; Neier, R. *Angew. Chem., Int. Ed.* **1998**, *37*, 358−360. Chen, C.-T.; Chao, S.-D.; Yen, K.-C.; Chen, C.-H.; Chou, I.-C.; Hon, S.-W. *J. Am. Chem. Soc.* **1997**, *119*, 11341−11342. Loh, T.-P.; Pei, J.; Koh, K. S.-V.; Cao, G.-Q.; Li, X.-R. *Tetrahedron Lett.* **1997**, *38*, 3465−3468. Yanagisawa, A.; Matsumoto, Y.; Nakashima, H.; Asakawa, K.; Yamamoto, H. *J. Am. Chem. Soc.* **1997**, *119*, 9319−9320. Carreira, E. M.; Lee, W.; Singer, R. A. *J. Am. Chem. Soc.* **1995**, *117*, 3649−3650. Yamada, Y. M. A.; Yoshikawa, N.; Sasai, H.; Shibasaki, M. *Angew. Chem., Int. Ed. Engl.* **1997**, *36*, 1871−1873.

(10) Fessner, W.-D.; Schneider, A.; Held, H.; Sinerius, G.; Walter, C.; Hixon, M.; Schloss, J. V. *Angew. Chem., Int. Ed. Engl.* **1996**, *35*, 2219−2221.

(11) Desper, J. M.; Breslow, R. *J. Am. Chem. Soc.* **1994**, *116*, 12081−12082. Koh, J. T.; Delaude, L.; Breslow, R. *J. Am. Chem. Soc.* **1994**, *116*, 11234−11240. Breslow, R.; Desper, J.; Huang, Y. *Tetrahedron Lett.* **1996**, *37*, 2541−4.

(12) Bell, R. P. *J. Chem. Soc.* **1937**, 1637−1640. Bell, R. P.; Lidwell, O. M. *Proc. R. Soc. London, Ser. A* **1940**, *176*, 88−121. Bell, R. P.; Smith, M. Y. *J. Chem. Soc.* **1958**, 1691−1696. Bell, R. P.; McTigue, P. T. *J. Chem. Soc.* **1960**, 2983−2994. Guthrie, J. P. *Can. J. Chem.* **1974**, *52*, 2037−2040.

(13) Nagorski, R. W.; Mizerski, T.; Richard, J. P. *J. Am. Chem. Soc.* **1995**, *117*, 4718−4719.

(14) (a) Amyes, T. L.; Richard, J. P. *J. Am. Chem. Soc.* **1992**, *114*, 10297−10302. (b) Amyes, T. L.; Richard, J. P. *J. Am. Chem. Soc.* **1996**, *118*, 3129−3141.

(15) Rios, A.; Richard, J. P. *J. Am. Chem. Soc.* **1997**, *119*, 8375−8376. Richard, J. P.; Williams, G.; Gao, J. *J. Am. Chem. Soc.* **1999**, *121*, 715−726.

(16) Halkides, C. J.; Frey, P. A.; Tobin, J. B. *J. Am. Chem. Soc.* **1993**, *115*, 3332−3333.

Scheme 2

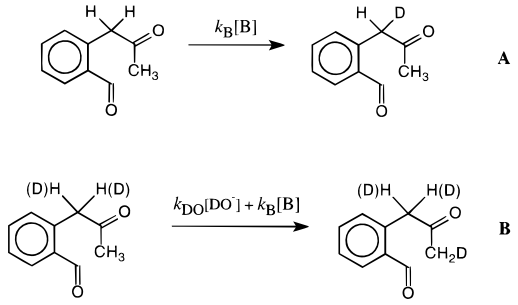

the appearance of **4** at 340 nm (usual method) or in some cases the disappearance of **1** at 256 nm. First-order rate constants, k_{obsd} (s^{-1}), were determined from the slopes of semilogarithmic plots of reaction progress against time, which were linear for at least three reaction halftimes. The values of k_{obsd} were reproducible to ±5%.

Rate constants for the slow reactions of **1** in the presence of low concentrations of 3-quinuclidinone at pH 8.8 (pH maintained with 10 mM pyrophosphate buffer) were determined from the initial velocity of formation of **4** during the first 6% of the reaction, with the assumption that the total change in absorbance at 340 nm is the same as that observed for the faster reaction of an equal concentration of **1** in the presence of high concentrations of 3-quinuclidinone.

HPLC product analyses were carried out as described in earlier work[17,18] with peak detection by a Waters 996 diode array detector.

Results

Figure S1 of the Supporting Information shows representative partial ^{1}H NMR spectra at 400 MHz of **1** recovered after its incubation in D_2O buffered with 3-quinuclidinone at pD 8.3 and 25 °C (I = 1.0, KCl). At early reaction times (Figure S1A) the disappearance of the singlet at 4.146 ppm due to the benzylic α-CH_2 group is accompanied by the appearance of a triplet at 4.118 ppm (J_{HD} = 2 Hz) due to the α-CHD group (Scheme 2A). At longer times (Figures S1B and S1C) the disappearance of the singlet at 2.327 ppm due to the α-CH_3 group is accompanied by the appearance of a triplet at 2.311 ppm (J_{HD} = 2 Hz) due to the α-CH_2D group (Scheme 2B). Semilogarithmic plots (not shown) of reaction progress against time according to eqs 3 and 4 were linear during exchange of 35% of the first proton of the α-CH_2 or the α-CH_3 group of **1**. The negative slopes of these plots are equal to $k_{obsd}/2$ (α-CH_2 group, eq 3) or $k_{obsd}/3$ (α-CH_3 group, eq 4), where k_{obsd} (s^{-1}) is the observed first-order rate constant for exchange of the *first* proton of the α-CH_2 group or the α-CH_3 group of **1** (Scheme 2).[16]

The slope of the linear plot of k_{obsd} (s^{-1}) for exchange for deuterium of the first proton of the α-CH_2 group of **1** against the concentration of the basic form of 3-quinuclidinone buffer in D_2O at pD 8.3 and 25 °C (I = 1.0, KCl) (not shown) is $k_B = 4.0 \times 10^{-2}$ M^{-1} s^{-1}, the second-order rate constant for exchange of the first proton of the α-CH_2 group of **1** catalyzed by 3-quinuclidinone (Scheme 2A).

Figure S2A of the Supporting Information shows the linear dependence of k_{obsd} (s^{-1}) for exchange for deuterium of the first proton of the α-CH_3 group of **1** on the concentration of the basic form of 3-quinuclidinone buffer in D_2O at pD = 7.7 or 8.3 and 25 °C (I = 1.0, KCl). The slope of this plot is $k_B = 3.4 \times 10^{-4}$ M^{-1} s^{-1}, the second-order rate constant for exchange of the first proton of the α-CH_3 group of **1** catalyzed by 3-quinuclidinone (Scheme 2B).

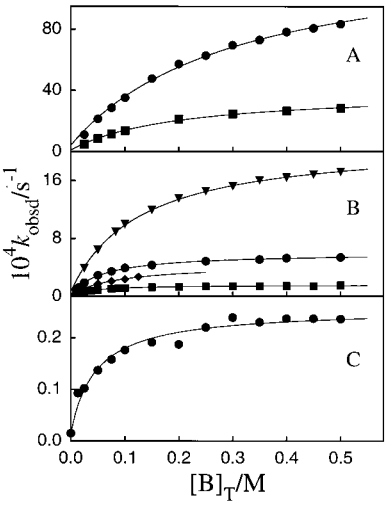

Figure 1. Dependence of k_{obsd} (s^{-1}) for the conversion of **1** to 2-naphthol (**4**) in H_2O on the total concentration of 3-substituted quinuclidine buffer at 25 °C (I = 1.0, KCl). The solid lines are the nonlinear least-squares fits of the data to eq 5, calculated as described in the text. (A) Catalysis by quinuclidine buffers. Key: (●), $[B]/[BH^+] = 1.0$; (■), $[B]/[BH^+] = 0.25$. (B) Catalysis by 3-quinuclidinol buffers. Key: (▼), $[B]/[BH^+] = 4$; (●), $[B]/[BH^+] = 1.0$; (■), $[B]/[BH^+] = 0.25$. Catalysis by 3-chloroquinuclidine buffers: (◆), $[B]/[BH^+] = 9.0$. (C) Catalysis by 3-quinuclidinone ($pK_{BH} = 7.5$),[19] $[B]/[BH^+] = 20$, at pH 8.8 in the presence of 10 mM pyrophosphate buffer.

Figure S2B of the Supporting Information shows the dependence of k_{obsd} (s^{-1}) for exchange for deuterium of the first proton of the α-CH_3 group of **1** on the concentration of deuterioxide ion in D_2O at 25 °C (I = 1.0, KCl). The slope of this correlation is $(k_{DO})_{ex} = 0.024$ M^{-1} s^{-1}, the second-order rate constant for exchange of the first proton of the α-CH_3 group of **1** catalyzed by deuterioxide ion. Signals for the aromatic protons of 2-naphthol (**4**) were detected by ^{1}H NMR spectroscopy during the course of these exchange reactions.

The aldol condensation reaction of **1** to give 2-naphthol (**4**) in 0.1 M potassium hydroxide in H_2O at 25 °C (I = 1.0, KCl) was monitored spectrophotometrically between 200 and 400 nm. The maximum decrease in absorbance due to the disappearance of **1** occurs at 256 nm, and the maximum increase in absorbance due to the formation of **4** occurs at 340 nm. Sharp isosbestic points were observed at 250, 267, 299, and 307 nm. No reaction intermediates were detected by HPLC analysis with peak detection at 256 nm during the conversion of **1** to **4** in the presence of 3-quinuclidinone buffer at pH 7.0.

First-order rate constants for the reaction of **1** to give **4** were determined spectrophotometrically by following the appearance of the product at 340 nm. Figure 1A shows the dependence of k_{obsd} (s^{-1}) for the conversion of **1** to **4** in H_2O on the concentration of quinuclidine buffers at 25 °C (I = 1.0, KCl) and Figure 1B shows the corresponding data for 3-quinuclidinol and 3-chloroquinuclidine buffers. Figure 1C shows the dependence of k_{obsd} (s^{-1}) for the conversion of **1** to **4** on the concentration of 3-quinuclidinone ($pK_{BH} = 7.5$)[19] in solutions that were buffered with 10 mM pyrophosphate at pH 8.8 and 25 °C (I = 1.0, KCl).

Figure S2B of the Supporting Information shows the dependence of k_{obsd} (s^{-1}) for the conversion of **1** to **4** on the concentration of hydroxide ion in H_2O and deuterioxide ion in D_2O at 25 °C (I = 1.0, KCl). The slopes of these plots are

(17) Richard, J. P.; Rothenberg, M. E.; Jencks, W. P. *J. Am. Chem. Soc.* **1984**, *106*, 1361−1372.
(18) Richard, J. P. *J. Am. Chem. Soc.* **1989**, *111*, 1455−1465.
(19) Gresser, M. J.; Jencks, W. P. *J. Am. Chem. Soc.* **1977**, *99*, 6963−6980.

Scheme 3

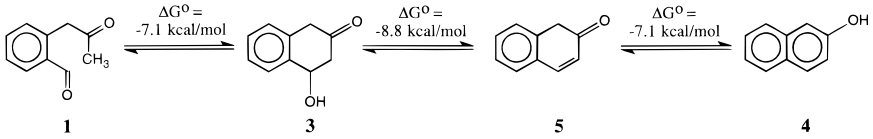

Scheme 4

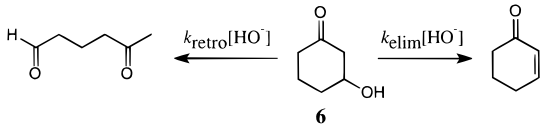

Scheme 5

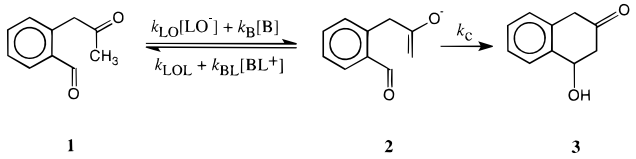

$(k_{HO})_{aldol} = 0.10\ M^{-1}\ s^{-1}$ and $(k_{DO})_{aldol} = 0.15\ M^{-1}\ s^{-1}$, the second-order rate constants for the reaction of **1** to give **4** catalyzed by hydroxide in H_2O and deuterioxide ion in D_2O, respectively.

Discussion

The observation of several isosbestic points when the intramolecular reaction of **1** to give 2-naphthol (**4**) was followed spectrophotometrically and the absence of the formation of any detectable intermediates as determined by HPLC analysis shows that there is no significant accumulation of **3** and **5** during these reactions. This is a consequence of the large overall thermodynamic driving force for conversion of **1** to **4** (ca. 23 kcal/mol) and the nearly equal division of the overall change in the standard Gibbs free energy between the three reaction steps, as determined in the elegant analysis of Guthrie et al. (Scheme 3).[5]

A rate constant ratio of $k_{elim}/k_{retro} = 3.5 \times 10^4$ has been estimated for the partitioning of **6** between elimination of water and retroaldol cleavage (Scheme 4).[5] An even larger value of this rate constant ratio is expected for the partitioning of **3** for which the elimination product **5** is extensively conjugated. Similarly, the thermodynamically favorable tautomerization of **5** to give **4** is expected to be much faster than the unfavorable addition of water to **5** to give **3**. We therefore conclude that the formation of **3** from **1** is effectively irreversible and rate-determining for the formation of **4**. Therefore, the observed rate constants for the reaction of **1** to give **4** determined in this work represent rate constants for the intramolecular aldol addition reaction of **1** to give **3** (Scheme 5).

The exchange for deuterium of the first proton of the α-CH_2 and α-CH_3 groups of **1** (Scheme 2) in D_2O at 25 °C ($I = 1.0$, KCl) was followed by ^1H NMR spectroscopy (Figure S1 of the Supporting Information). The second-order rate constants for catalysis of these exchange reactions by 3-quinuclidinone are $k_B = 4.0 \times 10^{-2}\ M^{-1}\ s^{-1}$ (α-CH_2 group) and $k_B = 3.4 \times 10^{-4}\ M^{-1}\ s^{-1}$ (α-CH_3 group). The difference in these rate constants is consistent with the known greater acidity of the benzylic protons of benzyl methyl ketone ($pK_a \approx 16$)[20] than of the protons of a single α-methyl group of acetone (statistically corrected $pK_a = 19.6$).[21]

Mechanism of Aldol Addition. The second-order rate constant for exchange for deuterium of the first proton of the α-CH_3 group of **1** catalyzed by deuterioxide ion in D_2O, $(k_{DO})_{ex} = 0.024\ M^{-1}\ s^{-1}$, is 6-fold smaller than $(k_{DO})_{aldol} = 0.15\ M^{-1}\ s^{-1}$ for the deuterioxide ion catalyzed aldol addition reaction of **1** in D_2O to give **3**. However, this value of $(k_{DO})_{aldol}$ is very close to the expected second-order rate constant for deprotonation of **1** by deuterioxide ion to give the acetone-like enolate **2**.[22,23] These results show that the deuterioxide ion catalyzed incorporation of deuterium into the α-CH_3 group of **1** is slower than both the deprotonation and aldol condensation reactions of **1**. This is consistent with the detection of **4** by ^1H NMR spectroscopy during these deuterium exchange reactions (see Results). By contrast, no **4** was detected by ^1H NMR spectroscopy during exchange for deuterium of 35% of the first proton of the α-CH_3 group of **1** in D_2O buffered with ≥0.10 M 3-quinuclidinone at pD ≈ 8.0. Therefore, under these reaction conditions, the partitioning of the enolate intermediate **2** strongly favors the formation of deuterium-labeled **1** over intramolecular aldol addition to give **3**.

These data show that the aldol addition reaction of **1** proceeds by a two-step mechanism in which lyoxide ion catalyzed deprotonation of **1** to give the enolate **2** is effectively irreversible and rate-determining for the formation of **3**, so that the observed second-order rate constant for lyoxide ion catalyzed aldol addition is essentially equal to the rate constant for deprotonation of **1**, $(k_{LO})_{aldol} = k_{LO}$ (Scheme 5). The observed second-order rate constant for deuterioxide ion catalyzed exchange of deuterium into the α-CH_3 group of **1** is *smaller* than that for deprotonation of **1**, $(k_{DO})_{ex} < k_{DO}$, because the enolate intermediate **2** undergoes ring closure (k_c) faster than its reprotonation by solvent D_2O ($k_c > k_{DOD}$, Scheme 5). By contrast, the strong buffer catalysis of proton transfer from **1** results in a change to fast and reversible proton transfer in the presence of high concentrations of 3-quinuclidinone buffer, $k_{BD}[BD^+] \gg k_c$ (Scheme 5), and a change in rate-limiting step for the overall aldol addition from proton transfer to form **2**, $k_{DO}[DO^-] + k_B[B]$, to the ring closure reaction of **2**, k_c (Scheme 5).

This change in rate-determining step for aldol addition is responsible for the downward curvature in the plots of k_{obsd} (s^{-1}) for the conversion of **1** to **3** in H_2O against the concentration of the buffer catalyst (Figure 1). At low buffer concentrations where proton transfer is rate-determining for the overall aldol addition ($k_c \gg k_{HOH} + k_{BH}[BH^+]$) the general base catalysis of proton transfer results in a linear dependence of k_{obsd} on buffer concentration (Scheme 5). However, on proceeding to high concentrations of the buffer catalyst the change in rate-limiting step from proton transfer to intramolecular addition of the

(20) Keeffe, J. R.; Kresge, A. J.; Yin, Y. *J. Am. Chem. Soc.* **1988**, *110*, 8201−8206.

(21) A pK_a of 19.3 has been determined for the carbon acidity of acetone (ref 2). A statistical correction gives $pK_a = 19.6$ for a single methyl group of acetone.

(22) A value of $k_{DO} = 0.32\ M^{-1}\ s^{-1}$ for deprotonation of acetone by deuterioxide ion in D_2O can be estimated from $k_{HO} = 0.22\ M^{-1}\ s^{-1}$ for deprotonation by hydroxide ion in H_2O (ref 23) and the secondary solvent isotope effect of $k_{DO}/k_{HO} = 1.46$ (ref 24). A statistical correction for the presence of two methyl groups at acetone gives $k_{DO} = 0.16\ M^{-1}\ s^{-1}$ for deprotonation of **1** by deuterioxide ion in D_2O.

(23) Chiang, Y.; Kresge, A. J.; Morimoto, H.; Williams, P. G. *J. Am. Chem. Soc.* **1992**, *114*, 3981−3982.

Table 1. Rate Constants for the Deprotonation of **1** by Brønsted Bases and the Reverse Protonation of **2** by Brønsted Acids, and Rate Constant Ratios for Partitioning of the Enolate Carbon of **2** between Protonation by Brønsted Acids and Intramolecular Aldol Addition in Water at 25 °C (I = 1.0, KCl) (Scheme 5)

Brønsted base	pK_{BH}[a]	[HO$^-$] (M)[b]	[B]/[BH$^+$]	k_B (M^{-1} s^{-1})[c]	k_{BH}/k_c (M^{-1})[c]	k_{BH} (M^{-1} s^{-1})[d]	k_{lim} (s^{-1})[e]	k_{lim}/k_{HO}[HO$^-$] = $k_c/k_{HOH}f$
	11.5	4.0×10^{-3}	1.0	8.8×10^{-2}	6.6	1.1×10^{7} [g]	1.3×10^{-2}	33
		1.0×10^{-3}	0.25	9.8×10^{-2}	6.1		4.0×10^{-3}	40
	10.0	6.3×10^{-4}	4.0	2.1×10^{-2}	40		2.1×10^{-3}	33
		1.6×10^{-4}	1.0	2.0×10^{-2}	34	6.5×10^{7} [g]	5.9×10^{-4}	37
		4.0×10^{-5}	0.25	2.1×10^{-2}	34		1.5×10^{-4}	38
	9.0	1.3×10^{-4}	9.0	5.7×10^{-3}	120	2.2×10^{8}	4.3×10^{-4}	33
	7.5	8.0×10^{-6}	20[h]	5.8×10^{-4}	450	8.1×10^{8}	2.6×10^{-5}	33

[a] Apparent acidity of the corresponding 3-substituted quinuclidinium cation at 25 °C and I = 1.0 (KCl). Data taken from ref 19. [b] The concentration of hydroxide ion was calculated from the solution pH as described in the Supporting Information. [c] Determined from the nonlinear least-squares fit of the data from Figure 1 to eq 5 (see text). [d] Calculated from the value of k_{BH}/k_c (M^{-1}) and $k_c = 1.8 \times 10^6$ s^{-1} (see text). [e] Limiting rate constant at high concentrations of buffer, calculated from the data in this table using eq 7 (see text). [f] Calculated from [HO$^-$] and k_{HO} = 0.10 M^{-1} s^{-1} for the deprotonation of **1** by hydroxide ion (see text). [g] Average of values at determined at different buffer ratios [B]/[BH$^+$]. [h] At pH 8.8 in the presence of 10 mM pyrophosphate buffer.

enolate to the carbonyl group ($k_c \ll k_{HOH} + k_{BH}$[BH$^+$]) results in a downward break and values of k_{obsd} that are independent of buffer concentration (Scheme 5).

$$k_{obsd} = \frac{k_{HO}[HO^-] + k_B f_B [B]_T}{1 + (k_{BH}/k_c) f_{BH} [B]_T} \quad (5)$$

Equation 5 gives the relationship between k_{obsd} (s^{-1}) for the overall aldol addition reaction of **1** to give **3** and the *total* concentration of the buffer catalyst, $[B]_T$ (Figure 1). This equation was derived for the mechanism shown in Scheme 5, with the simplifying assumption that the barrier for reprotonation of the enolate intermediate **2** by solvent is significantly larger than the barrier to intramolecular addition of the enolate to the carbonyl group ($k_{HOH} \ll k_c$, see following section). The known parameters in eq 5 are $k_{HO} = (k_{HO})_{aldol}$ = 0.10 M^{-1} s^{-1}, the observed second-order rate constant for hydroxide ion catalysis of the aldol addition reaction of **1** with rate-determining deprotonation (see Results section); [HO$^-$], determined from the observed pH of the solution (Table 1); and f_B and f_{BH}, the fraction of the buffer present in the basic (B) and acidic forms (BH$^+$), respectively (Table 1). The nonlinear least-squares fits of the data in Figure 1 to eq 5 gave the rate constants k_B (M^{-1} s^{-1}) and the partitioning ratios k_{BH}/k_c (M^{-1}) given in Table 1. The uncertainties in k_B and k_{BH}/k_c, estimated from the range of the values determined for catalysis by a single buffer at different acid/base ratios are ±10% and ±20%, respectively (Table 1).

Enolate Addition to the Carbonyl Group. The reaction coordinate profile in Scheme 6 shows that the difference in the activation barriers for partitioning of **2** between protonation by solvent water (k_{HOH}) and intramolecular addition of the enolate carbon to the carbonyl group (k_c), $\Delta\Delta G^{\ddagger}$, is given by the difference in the activation barriers for the overall aldol addition reaction of **1** when proton transfer ($\Delta G^{\ddagger}_{HO}$) and enolate addition are rate-determining ($\Delta G^{\ddagger}_{lim}$), so that $k_c/k_{HOH} = k_{lim}/k_{HO}$[HO$^-$] (eq 6),

$$\frac{k_{lim}}{k_{HO}[HO^-]} = \frac{k_c}{k_{HOH}} \quad (6)$$

Scheme 6

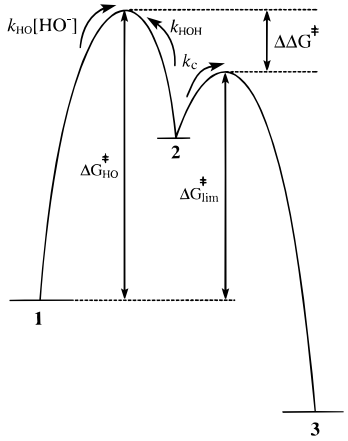

where k_{lim} (s^{-1}) is the limiting first-order rate constant for the overall aldol addition reaction of **1** to give **3** in the presence of high concentrations of a buffer catalyst at a specified pH. At high concentrations of buffer, k_{BH}[BH$^+$] ≫ k_c, k_c is fully rate-determining, so that $k_{obsd} = k_{lim}$ and $\Delta G^{\ddagger}_{obsd} = \Delta G^{\ddagger}_{lim}$ (Scheme 6). Equation 7 is the limiting form of eq 5 at high concentrations of buffer where $k_{obsd} = k_{lim}$ and f_B/f_{BH} = [B]/[BH$^+$].

$$k_{lim} = \frac{k_B([B]/[BH^+])}{(k_{BH}/k_c)} \quad (7)$$

The values of k_B, k_{BH}/k_c, and [B]/[BH$^+$] in Table 1 were substituted into eq 7 to give values of k_{lim}. These values of k_{lim} were then combined with k_{HO} = 0.10 M^{-1} s^{-1} and [HO$^-$] according to eq 6 to give the values of k_c/k_{HOH} in Table 1. The values of k_c/k_{HOH} determined for several pH values and buffer catalysts range from 33 to 40 with an average value of $k_c/k_{HOH} = 35 \pm 5$.

The enolate of acetone was generated by laser flash photolysis and the rate constant for its protonation by solvent water determined as $k_{HOH} = 5.0 \times 10^4$ s^{-1}.[25] The rate constants for

(24) Pocker, Y. *Chem. Ind.* **1959**, 1383−1384.

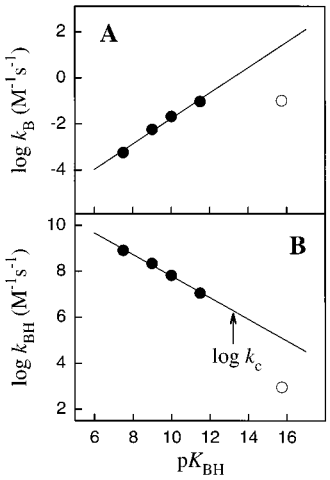

Figure 2. Brønsted correlations of rate constants for reversible proton transfer from **1** to 3-substituted quinuclidines (pK_{BH} = 7.5−11.5)[19] in H_2O at 25 °C (I = 1.0, KCl). (A) Brønsted correlation for deprotonation of **1** by 3-substituted quinuclidines. Values of k_B (M^{-1} s^{-1}) were taken from Table 1. The open circle corresponds to k_{HO} = 0.10 M^{-1} s^{-1} for deprotonation of **1** by hydroxide ion (see text). (B) Brønsted correlation for protonation of **2** by 3-substituted quinuclidinium cations. Values of k_{BH} (M^{-1} s^{-1}) were taken from Table 1. The open circle corresponds to (k_{HOH}/55 M) = 900 M^{-1} s^{-1} for protonation of **2** by water (see text).

hydroxide ion catalyzed deprotonation of the α-CH_3 group of **1** (k_{HO} = 0.10 M^{-1} s^{-1}, see above) and a single α-CH_3 group of acetone (k_{HO} = 0.11 M^{-1} s^{-1})[23] are nearly identical, so that it is reasonable to assume that the rate constant for the reverse protonation of the acetone-like enolate **2** by solvent water is the same as that for the enolate of acetone. Therefore, the rate constant ratio k_c/k_{HOH} = 35 for the partitioning **2** can be combined with k_{HOH} = 5.0 × 10^4 s^{-1} to give k_c = 1.8 × 10^6 s^{-1} for intramolecular addition of the enolate carbon of **2** to the carbonyl group. This can be compared with the estimated second-order rate constant for bimolecular addition of the acetone enolate to benzaldehyde, $(k_c)_{bi}$ = 2.4 × 10^4 M^{-1} s^{-1},[4] to give an approximate effective molarity of 75 M for the intramolecular enolate addition reaction of **2**.[26] Effective molarities of 0.1−50 M have been reported for intramolecular deprotonation of α-carbonyl carbon,[26,27] and the range of effective molarities must be the same for reactions in the reverse direction of enolate protonation. This shows that there is, at best, only a modest advantage to intramolecular addition of an enolate to the carbonyl group over its intramolecular protonation by Brønsted acids.

Brønsted Relationships. The rate constant ratios k_{BH}/k_c (M^{-1}) for partitioning of the enolate **2** between protonation by buffer acids and intramolecular aldol addition were combined with k_c = 1.8 × 10^6 s^{-1} (see above) to give absolute values of k_{BH} (M^{-1} s^{-1}) (Table 1). Figure 2 shows Brønsted correlations of rate constants for deprotonation of **1** by 3-substituted quinuclidines, k_B (Figure 2A), and the reverse protonation of **2** by the corresponding tertiary ammonium cations, k_{BH} (Figure 2B), with the pK_a of the buffer catalyst, pK_{BH}. The solid lines show the fits of the data to eqs 8 and 9 which give β = 0.55 (Figure 2A) and α = 0.47 (Figure 2B).

The Brønsted correlations determined in this work for the deprotonation of **1** (eq 8) and the microscopic reverse protonation of **2** (eq 9) meet two requirements for an internally consistent set of data: (1) The sum of the Brønsted exponents obtained from eqs 8 and 9 is $\alpha + \beta$ = 1.02, which is in agreement with the required value of 1.00 for the logarithmic change in the overall equilibrium constant with changing basicity of the buffer catalyst, pK_{BH}. (2) The *y*-intercepts given by eqs 8 and 9 correspond to the rate constants for deprotonation of **1** and the reverse protonation of **2** by a hypothetical buffer catalyst of pK_{BH} = 0, and the difference of these intercepts, $\log(k_{BH}/k_B)_0$ = 19.8, is in agreement with the required value of 19.6, which is the difference between pK_{BH} = 0 for this hypothetical buffer catalyst and pK_a = 19.6 for the α-CH_3 group of **1**.[21]

$$\log k_B = -7.3 + 0.55pK_{BH} \quad (8)$$

$$\log k_{BH} = 12.5 - 0.47pK_{BH} \quad (9)$$

The acidity of a hypothetical tertiary ammonium cation that exhibits the same electrophilic reactivity toward **2** in an intermolecular reaction (k_{BH} = 1.8 × 10^6 M^{-1} s^{-1}) as the benzaldehyde carbonyl group in an intramolecular reaction (k_c = 1.8 × 10^6 s^{-1}) can be calculated from eq 9 as pK_{BH} = 13.3. By contrast, the acidity of a hypothetical tertiary ammonium cation that exhibits the same electrophilic reactivity toward **2** in a bimolecular reaction as the benzaldehyde carbonyl group in a bimolecular reaction ($k_{BH} = (k_c)_{bi}$ = 2.4 × 10^4 M^{-1} s^{-1})[4] is pK_{BH} = 17.3. The higher pK_a estimated for a hypothetical Brønsted acid with the same chemical reactivity as the benzaldehyde carbonyl group in inter- (pK_{BH} = 17.3) compared to intramolecular (pK_{BH} = 13.3) reactions is a direct consequence of the effective molarity of ≈75 M for intramolecular addition of the enolate carbon of **2** to the benzaldehyde carbonyl group (see above).

Deuterioxide Ion Catalyzed Exchange. The observation that buffer catalysts result in a limiting ca. 35-fold increase in k_{obsd} for the overall aldol addition reaction of **1** (Table 1 and Figure 1) requires that k_c for the intramolecular addition reaction of **2** be 35-fold larger than k_{HOH} for its protonation by solvent water (eq 6). The corresponding partitioning ratio in D_2O should be even larger due to a primary isotope effect on the protonation of **2** by solvent, so that $k_c/k_{DOD} > 35$. This would require that deuterium exchange of the protons of the α-CH_3 group of **1** occur less than once every 35 times that **2** is generated by deprotonation of **1** by deuterioxide ion, so that almost all the deprotonation events result in ring closure to give the aldol adduct **3**, and $k_{DO} = (k_{DO})_{aldol}$ = 0.15 M^{-1} s^{-1}. Therefore, the rate constant for deuterioxide ion catalyzed exchange of the first proton of the α-CH_3 group of **1** through the enolate intermediate **2** is expected to be $(k_{DO})_{ex} \leq k_{DO}/35$ = 4.3 × 10^{-3} M^{-1} s^{-1}. This is significantly smaller than the *observed* value of $(k_{DO})_{ex}$ = 0.024 M^{-1} s^{-1}. We conclude that while the deuterioxide ion catalyzed exchange of the protons of the α-CH_3 group of **1** [$(k_{DO})_{ex}$ = 0.024 M^{-1} s^{-1}] is significantly slower than deprotonation of **1** [$(k_{DO})_{aldol}$ = 0.15 M^{-1} s^{-1}], it is also unexpectedly fast. The mechanism for this exchange reaction is discussed further in the Supporting Information.

Electrophilicity of Brønsted Acids and the Carbonyl Group. A comparison of k_c for the intramolecular aldol addition reaction of **2** with the rate constants for protonation of **2** (Figure 2B) shows that Brønsted acids may be either more or less reactive than a benzaldehyde carbonyl group. The importance of the intrinsic reaction barrier and thermodynamic driving force in the determination of these relative rate constants is examined in Table 2, which summarizes rate and equilibrium constants for reactions of the acetone-like enolate **2** with Brønsted acids

(25) Chiang, Y.; Kresge, A. J.; Tang, Y. S.; Wirz, J. *J. Am. Chem. Soc.* **1984**, *106*, 460−462.
(26) Kirby, A. J. *Adv. Phys. Org. Chem.* **1980**, *17*, 183−278.
(27) Richard, J. P. *J. Am. Chem. Soc.* **1984**, *106*, 4926−4936.

Table 2. Rate and Equilibrium Constants for Reactions of the Acetone-like Enolate **2** with Brønsted Acids and a Benzaldehyde-type Carbonyl Group in Water at 25 °C (I = 1.0, KCl)

reaction	pK_{BH}	K^a	k_f	k_r	Λ^b (kcal/mol)	log k_0^c
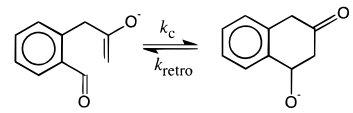		3.3×10^8 [d]	1.8×10^6 (s^{-1})[e]	5.5×10^{-3} (s^{-1})[f]	14.1	2.4
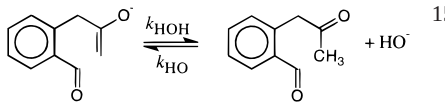	15.7	5.0×10^5 (M)[g]	5.0×10^4 (s^{-1})[h]	0.10 (M^{-1} s^{-1})[i]	14.7	2.0
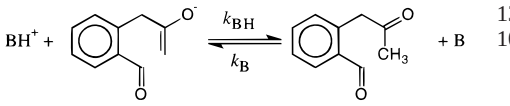	13.3[j] 10.8[l]	1.8×10^6 [g] 3.3×10^8	1.8×10^6 (M^{-1} s^{-1}) 1.4×10^7 (M^{-1} s^{-1})[m]	1.0 (M^{-1} s^{-1})[k] 4.3×10^{-2} (M^{-1} s^{-1})[k]	12.8 12.9	3.4 3.3

[a] Equilibrium constant for the reaction of **2** as shown, given by $K = k_f/k_r$. [b] Marcus intrinsic barrier (kcal/mol) for the reaction of **2**, calculated from the rate and equilibrium constants using eq 10. [c] Logarithm of the Marcus intrinsic rate constant for the reaction of **2**, calculated from intrinsic barrier Λ using eq 11. [d] Calculated from $K = 1.2 \times 10^5$ for reaction of **2** to give the ketol **3** [ref 5], pK_a = 19.6 for the α-CH_3 protons of **1** [ref 21], and pK_a = 15.9 for the ketol hydroxyl of **3** [ref 5]. [e] $k_c = 1.8 \times 10^6$ s^{-1}, see text. [f] Calculated as $k_r = k_f/K$. [g] Calculated as $K = k_f/k_r$. [h] Data for enolate of acetone [ref 25]. [i] $k_{HO} = (k_{HO})_{aldol}$, data from this work. [j] Acidity of hypothetical tertiary ammonium cation for which $k_c = k_{BH} = 1.8 \times 10^6$ M^{-1} s^{-1} (see text). [k] Calculated from pK_{BH} using eq 9. [l] Acidity of hypothetical tertiary ammonium cation for which $K = 3.3 \times 10^8$ for protonation of **2** is equal to that for intramolecular addition of **2** to the carbonyl group, calculated using pK_a = 19.6 for the α-CH_3 protons of **1** [ref 21]. [m] Calculated as $k_f = Kk_r$.

and the benzaldehyde carbonyl group. Marcus intrinsic barriers Λ (kcal/mol, Table 2) for the hypothetical thermoneutral reactions ($\Delta G° = 0$) were estimated from the appropriate rate and equilibrium constants using eq 10 (derived at 298 K).[4,28−30] The Marcus intrinsic rate constants for these thermoneutral reactions, k_0, were then estimated from these intrinsic barriers using eq 11 (derived at 298 K).

$$\log k_{obsd} = \frac{1}{1.36}\left\{17.44 - \Lambda\left(1 - \frac{1.36 \log K}{4\Lambda}\right)^2\right\} \quad (10)$$

$$\log k_0 = 12.8 - \frac{\Lambda}{1.36} \quad (11)$$

The data in Table 2 show that the enolate **2** has a greater reactivity toward the benzaldehyde carbonyl group ($k_c = 1.8 \times 10^6$ s^{-1}, Table 2) than toward solvent water ($k_{HOH} = 5 \times 10^4$ s^{-1}), but the similar values of k_o for these reactions show that this difference in reactivity is due mainly to the larger thermodynamic driving force for carbonyl addition. As noted by Guthrie in an earlier study of related intermolecular and intramolecular aldol addition reactions,[4,5] the intrinsic barriers for reaction of an acetone-like enolate with a benzaldehyde carbonyl group (Λ = 14.1 kcal/mol, Table 2) and solvent water (Λ = 14.7 kcal/mol, Table 2) are very similar. The larger intrinsic barrier for protonation of **2** by solvent water (Λ = 14.7 kcal/mol) than by a tertiary ammonium cation of pK_{BH} =13.3 with the same reactivity toward **2** (Λ = 12.8 kcal/mol) is generally observed for proton transfer at α-carbonyl carbon, and is manifested as negative deviations of rate constants for solvent-catalyzed proton transfer at carbon from Brønsted correlations (Figure 2, open symbols). Possible explanations for the deviation of the point for lyoxide ion from rate-equilibrium correlations have been discussed elsewhere.[27,30−33]

The smaller rate constant for the intramolecular aldol addition reaction of **2** ($k_c = 1.8 \times 10^6$ s^{-1}) compared to protonation of **2** by a tertiary ammonium cation whose pK_{BH} of 10.8 was chosen so that the two reactions would have the same thermodynamic driving force ($k_{BH} = 1.4 \times 10^7$ M^{-1} s^{-1}) shows that there is a larger intrinsic barrier for the former reaction (Table 2).

Table 3. Intrinsic Rate Constants for Proton Transfer and Nucleophilic Addition Reactions of Hard and Soft Acids and Bases in Water

		Intrinsic Rate Constant	
		Acid	
		HOH (Hard)	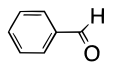 (Soft)
Base	$^-$OH (Hard)	$k_o = 4 \times 10^9$ M^{-1} s^{-1} [a]	$k_o = 6 \times 10^3$ M^{-1} s^{-1} [b]
	 (Soft)	$k_o = 100$ s^{-1} [c]	$k_o = 250$ s^{-1} [d]

[a] Data from refs 36 and 37. [b] Reference 38. [c] Calculated from log k_0 = 2.0 (Table 2). [d] Calculated from log k_0 = 2.4 (Table 2).

Table 3 compares the Marcus intrinsic rate constants, k_0, for the reactions of "hard" (water and hydroxide ion) and "soft" (carbonyl group and enolate ion) Lewis/Brønsted acids and bases. These data follow the general trend that reactions between soft acids and soft bases are intrinsically faster than reactions between hard and soft pairs of acids and bases.[34,35]

1. The intrinsic reactivity of the hard base hydroxide ion with the hard acid water, $k_0 = 4 \times 10^9$ M^{-1} s^{-1},[36,37] is much larger than that of the "soft" enolate ion with water, $k_0 = 100$ s^{-1}.

(28) Marcus, R. A. *J. Phys. Chem.* **1968**, *72*, 891−899.
(29) Marcus, R. A. *J. Am. Chem. Soc.* **1970**, *91*, 7224−7225.
(30) Kresge, A. J. *Chem. Soc. Rev.* **1973**, *2*, 475−503.
(31) Jencks, W. P.; Brant, S. R.; Gandler, J. R.; Fendrich, G.; Nakamura, C. *J. Am. Chem. Soc.* **1982**, *104*, 7045−7051.
(32) Pohl, E. R.; Hupe, D. J. *J. Am. Chem. Soc.* **1978**, *100*, 8130−8133.
(33) Washabaugh, M. W.; Jencks, W. P. *J. Am. Chem. Soc.* **1989**, *111*, 683−692.
(34) *Hard and Soft Acids and Bases*; Pearson, R. G., Ed.; Dowden, Hutchinson and Ross: Stroudsberg, PA, 1973.
(35) Pearson, R. G. *Chemical Hardness*; John Wiley & Sons: New York, 1997; p 208.
(36) Meiboom, S. *J. Chem. Phys.* **1961**, *34*, 375−388.
(37) Loewenstein, A.; Szöke, A. *J. Am. Chem. Soc.* **1962**, *84*, 1151−1154.

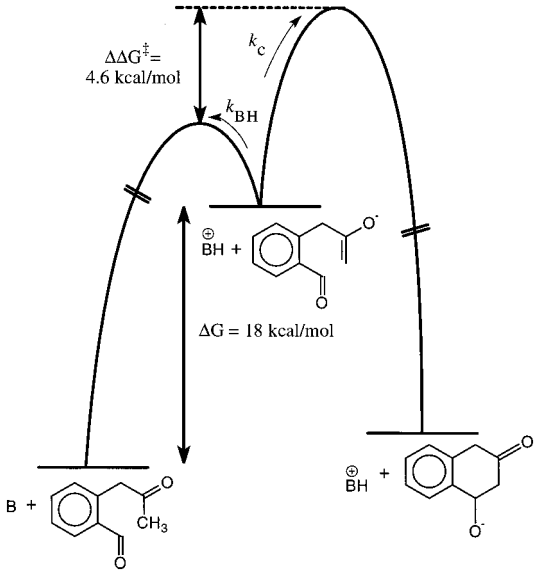

Figure 3. Free energy reaction coordinate profile for catalysis of the intramolecular aldol addition reaction of **1** by 1.0 M of a Brønsted base catalyst of $pK_{BH} = 6$. The profile was constructed as described in the text.

2. The requirement for rehybridization and electronic reorganization at the benzaldehyde carbonyl group upon addition of nucleophiles results in a smaller intrinsic rate constant for reaction of benzaldehyde with hydroxide ion ($k_0 = 6 \times 10^3$ M^{-1} s^{-1}) compared with proton transfer from water to hydroxide ion ($k_0 = 4 \times 10^9$ M^{-1} s^{-1}). This same requirement for rehybridization and electronic reorganization at the benzaldehyde carbonyl group might have been expected to result in a decrease in the intrinsic rate constant for its reaction with **2**, compared with the intrinsic rate constant for the reaction of water with **2**. However, the intrinsic rate constant for protonation of the acetone-like enolate **2** (a soft base) by the hard acid water, $k_0 = 100$ s^{-1}, is slightly *smaller* than $k_o = 250$ s^{-1} for addition of **2** to a benzaldehyde-type carbonyl group (a soft acid) (Table 3). We suggest that the expected decrease in the intrinsic rate constant (increase in the intrinsic barrier Λ) for the latter reaction is masked by a compensating stabilization of the transition state from favorable interactions between the "soft" Lewis acid−base pair.[34,35] Therefore, a simple consideration of the barriers to geometric and electronic rearrangement may not be sufficient to model the activation barrier for reactions,[39] because these barriers are also affected by developing covalent/ionic bonding interactions between the reacting atoms in the transition state.

Enzymatic Catalysis of Aldol Addition. Figure 3 shows a free energy reaction coordinate profile for reaction of a general base catalyst of $pK_{BH} = 6$ and a ketone with an aldehyde to give the products of an intramolecular aldol addition reaction. This profile was constructed using rate constants for a catalyst of $pK_{BH} = 6$ calculated from eq 8 ($\log k_B = -4.0$) and eq 9 ($\log k_{BH} = 9.7$), $\log k_c = 6.3$, and $pK_a = 19.6$ as the carbon acidity of the ketone.[21] This figure depicts the relative barriers for partitioning of an enolate ion between intramolecular addition to the carbonyl group and intermolecular protonation by Brønsted acids that have been determined in this work, $\Delta\Delta G^{\ddagger} = 4.6$ kcal/mol. Similar free energy profiles are expected for termolecular aldol addition reactions, except that in this second case partitioning of the enolate between *intermolecular* reactions with Brønsted acids and the carbonyl group might show a small increase in k_c for carbonyl addition, relative to k_{BH}, due to the larger effective molarity of ca. 75 M for the former reaction (see above).

The value of $pK_{BH} = 6$ was chosen for the catalytic base in Figure 3 because enzymes usually maintain full catalytic activity throughout the physiological pH range, which requires $pK_a < 7$ for essential basic residues. The profile in Figure 3 demonstrates two important roles of Class II aldolases in stabilization of the transition state for aldol addition reactions.

1. Interactions that stabilize the enolate relative to the keto form of the substrate will result in a decrease in the ca. 18 kcal/mol barrier to enolization and they will also stabilize the enolate-ion-like transition state for the rate-determining addition of the enolate to a carbonyl electrophile (k_c, Figure 3). Such interactions might include the formation of a strong, single-potential, hydrogen bond between the enzyme and the enolate ion,[40] or binding interactions which are expressed at the enzyme-enolate complex, but not at the enzyme-ketone complex.[41]

2. Specific stabilization of the rate-determining transition state for addition of the enolate to the carbonyl electrophile from electrophilic catalysis by an acidic amino acid side chain or a metal cation. This could lower the overall barrier to the general-base-catalyzed aldol addition, for which the enolate addition step is rate-determining, by 4−5 kcal/mol, until the point where substrate deprotonation again becomes rate-determining for the overall aldol addition (Figure 3). For the reaction shown in Figure 3, this would correspond to a net rate acceleration of ca. 2000-fold.

Acknowledgment. This work was supported by grants GM 39754 and 47307 from the National Institutes of Health. We thank Dr. Tadeusz Mizerski for the synthesis of **1** and Dr. Tina L. Amyes for helpful discussion.

Supporting Information Available: Experimental details of the following: (a) Procedures for the synthesis of **1**. (b) Procedures for the preparation of solutions used for kinetic studies. (c) Procedures for monitoring the deuterium exchange reactions of **1**. A discussion of the mechanism for the deuterioxide ion catalyzed exchange of the protons of the α-CH_3 group of **1**. Figure S1: Representative ^1H NMR spectra obtained during exchange for deuterium of the protons of the α-CH_2 and α-CH_3 groups of **1**. Figure S2: Dependence of k_{obsd} (s^{-1}) for exchange for deuterium of the first proton of the α-CH_3 group of **1** on the concentration of the basic form of 3-quinuclidinone buffer and deuterioxide ion in D_2O; dependence of k_{obsd} (s^{-1}) for the conversion of **1** to **4** on the concentration of hydroxide ion in H_2O and deuterioxide ion in D_2O. This material is available free of charge via the Internet at http://pubs.acs.org.

JA9900297

(38) Calculated by interpolation of the linear plot of rate ($\log k_{HO}$) and equilibrium ($\log K_{HO}$) constants for addition of hydroxide ion to ring-substituted benzaldehydes in water: McClelland, R. A.; Coe, M. *J. Am. Chem. Soc.* **1983**, *105*, 2718−2725. The least-squares correlation line for these data is $\log k_{HO} = 3.8 + 0.81 \log K_{HO}$.

(39) Guthrie, J. P. *J. Am. Chem. Soc.* **1997**, *119*, 1151−1152.

(40) Gerlt, J. A.; Kozarich, J. W.; Kenyon, G. L.; Gassman, P. G. *J. Am. Chem. Soc.* **1991**, *113*, 9667−9669. Gerlt, J. A.; Gassman, P. G. *J. Am. Chem. Soc.* **1992**, *114*, 5928−5934. Gerlt, J. A.; Gassman, P. G. *J. Am. Chem. Soc.* **1993**, *115*, 11552−11568. Gerlt, J. A.; Gassman, P. G. *Biochemistry* **1993**, *32*, 2, 11943−11952.

(41) Jencks, W. P. In *Adv. Enzymol. Relat. Areas Mol. Biol.*; Meister, A., Ed.; John Wiley and Sons: 1975; Vol. 43; pp 219−410.